Topic Introduction

Live Cell Imaging of Yeast

Daniel R. Rines, Dominik Thomann, Jonas F. Dorn, Paul Goodwin, and Peter K. Sorger

INTRODUCTION

The development of cloning vectors for green fluorescent protein (GFP) and the simplicity of yeast reverse genetics allow straightforward labeling of yeast proteins in living cells. Budding and fission yeast are therefore attractive organisms in which to study dynamic cellular processes such as growth, cell division, and morphogenesis using live cell fluorescence microscopy. This article focuses on methods to culture, mount, and observe budding yeast cells using three-dimensional (3D) microscopy, but the methods are broadly applicable to other types of cells and other imaging techniques. The emphasis is on 3D imaging, because yeast cells are roughly spherical, and most organelles in yeast move in three dimensions. Three-dimensional imaging also makes it possible to apply image restoration methods (e.g., deconvolution) to obtain sharper images with better definition. This is important, because yeast cells are small (haploid *Saccharomyces cerevisiae* cells have a diameter of ~4–5 µm) relative to the resolution of even the best optical microscope (~0.25 µm).

BACKGROUND

Making a live cell movie involves trade-offs between the number of optical slices collected per time point, the brightness of each slice, the sampling frequency, and the movie's duration. Properties of the sample and limitations in the imaging system link these variables together in a complex fashion. One unavoidable limitation is the total amount of light to which a live yeast cell can be exposed without causing photobleaching or disrupting critical cellular processes. Upon extended illumination, chemical and GFP-based fluorophores become sufficiently bleached that they can no longer be detected above background. Moreover, cells are sensitive to light and will die, or they will arrest cell division if overexposed. Like other cell types, *S. cerevisiae* appears to be more sensitive to blue light (~420–480 nm) than to near-ultraviolet (UV) or infrared irradiation. This sensitivity creates a serious problem, because it overlaps the excitation wavelength for most variants of GFP. The practical impact of photobleaching and phototoxicity is that the investigator must limit the frequency of sampling, the number of slices per time point, and the duration of a movie so that the cells remain below their exposure limit.

Microscopes are subject to fundamental limitations in optical resolution, acquisition speed, and the signal-to-noise response, all of which are of practical interest in live cell experiments and must be balanced to achieve the highest-quality results. For instance, short exposures increase the sampling rate but decrease the signal-to-noise ratio (SNR) and effective image resolution. Long exposures improve SNR and resolution but increase photodamage and reduce the frequency of sampling. All microscopy, whether fixed or live cell, must begin with high-quality samples, accurately aligned optics, and mounting techniques that minimize aberrations in image formation. However, there is no single best way to set the exposure time, section thickness, duration, or other critical features of a live cell movie. Instead, the limitations of the sample and the instrument must be evaluated with respect to the goals of an individual experiment. For example, if a dynamic process is monitored with bright, 3D stacks collected every 5 sec over a period of 5 min, the acquisition of such a movie would cause significant photobleaching. This would be a valid way to examine rapid processes in mitosis but would not allow the overall timing of cell division to be elucidated. For cell cycle studies, phototoxicity negatively affects cell growth. The intensity of illumination and frequency of sampling must therefore be minimized,

Adapted from *Live Cell Imaging*, 2nd edition (ed. Goldman et al.).
CSHL Press, Cold Spring Harbor, NY, USA, 2010.
Cite as: Cold Spring Harb Protoc; 2011; doi:10.1101/pdb.top065482

with a consequent reduction in temporal resolution. This article briefly discusses the physics that underlie the limitations inherent in optical microscopy and the ways live cell imaging can be optimized within these limits.

SPATIAL AND TEMPORAL RESOLUTION

The two most frequent questions in microscopy concern resolution: What is the smallest object that can be detected? How close can two objects be and remain distinct in the image? The resolution of optical microscopes is limited by the diffraction of light as it passes through circular apertures in the objective lens and other optical elements. All microscopes are subject to this effect, which is typically referred to as the "diffraction limit." Light from a point source object, which is necessarily below the diffraction limit, is spread out to generate a blurred distribution known as the point-spread function (PSF). This distribution is narrower in the *x-y* plane than along the *z* axis and its central portion resembles an elongated ellipse standing on end (Fig. 1A,B). Occasionally, the PSF will be referred to as the "impulse response" of the microscope because it represents the output in response to a point source impulse or input. It turns out to be remarkably useful to examine the PSF of an objective lens under real imaging conditions (see below). Imaging small point sources in a real biological sample (e.g., fluorescently tagged spindle pole bodies) can be used to confirm the quality of images by checking that the blurred image resembles a symmetric PSF. Asymmetry in the PSF along the *z* axis is known as "spherical aberration" and is only corrected by selecting an immersion oil with a different refractive index (see the section on Refractive Index Matching Using Immersion Media). Normally, the elliptical shape would be seen along the *z* axis (Fig. 1B) as well as a bright circle with multiple concentric rings of rapidly decreasing amplitude in the *x-y* plane (Fig. 1C). The central part of this pattern is referred to as the Airy disk and contains ~85% of the total light; the concentric rings contain the remaining 15%. Restoration, or deconvolution microscopy, uses information about the PSF to increase the sharpness of an image by attempting to re-create the original object from its blurred image.

Spatial resolution is typically defined using the Rayleigh criterion, in which two point sources are considered to be distinctly resolvable when they are separated by no less than a distance d_{xy}^{R} from each other in the *x-y* plane (perpendicular to the optical axis) and d_{z}^{R} in the *z* plane (parallel to the optical axis) (Inoue 1995):

$$d_{xy}^{R} = 0.61\frac{\lambda}{NA}, d_{z}^{R} = 2\frac{\lambda n}{NA^{2}}.$$

The Rayleigh distance is the point at which the first minimum in the diffraction-induced pattern (Fig. 2A) of one point source overlaps the maximum in the second (Fig. 2B,C). Resolution increases

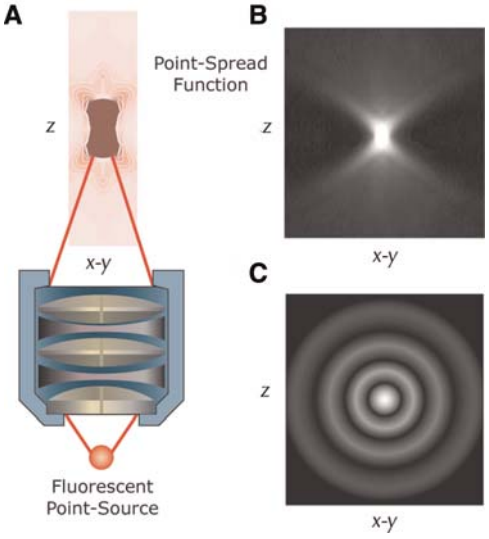

FIGURE 1. Point-spread function (PSF). (*A*) Light collected from a fluorescent point source (e.g., a small bead) is smeared. The smearing effect is a well-understood phenomenon and can be modeled computationally (Thomann et al. 2002). (*B*) Complex pattern of smearing is commonly referred to as the PSF and is a characteristic of lens magnification, construction, immersion medium, coverglass, and any cellular components between the focal plane and lens. A perfect PSF will have symmetric cones of light *above* and *below* the point source. This effect is best observed by optical *z* sectioning through a single point source. Light from the *z* stack, when viewed directly from the side, generates the pattern or distribution shown here. (*C*) The large circular pattern represents a view of the PSF from *above* and is commonly referred to as an Airy disk. The signal intensity is represented by the density shading.

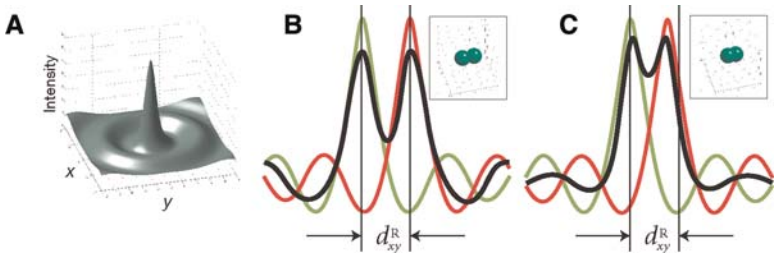

FIGURE 2. Rayleigh resolution criteria. Green spheres in insets represent two identical point sources in close proximity. Green curves show fluorescent intensity of one point source; red curves represent intensity of other source; black curves show the cumulative signal from both point sources. (*A*) A three-dimensional representation of an Airy distribution. Zeroth order is represented by the large peak in the center, and successive orders occur in the circular radial bands. (*B*) When two objects are in close proximity to one another where the Airy patterns overlap by <42% of the maximal intensities, the objects are individually resolvable (equal intensity objects). Rayleigh resolution limit (dR) represents the minimum distance the two objects can be to each other. (*C*) If the objects move together with >42% of their maximal intensity overlapping, the ability to resolve the objects as distinct is no longer possible. Notice that the two maxima are closer than the Rayleigh resolution limit.

with higher numerical aperture (NA) in the objective lens and decreases with higher-wavelength (*A*) or refractive index (*n*) values. Thus, with a 100× 1.4 NA objective, the Rayleigh resolution limit with green light is ~250 nm in the *x*-*y* plane and ~700 nm in the *z* plane. It is important to note that this resolution can only be achieved under optically ideal circumstances in which spherical aberration has been minimized (see the section on Refractive Index Matching Using Immersion Media). Image restoration methods are designed to compensate for optical blurring but not for sample preparation problems or poor instrument alignment. Fortunately, yeast cells are sufficiently small that we need not concern ourselves with sample-induced light scattering and depth-dependent aberrations that normally complicate image collection when working with tissues and other thick specimens.

In live cell imaging, we are also concerned with temporal resolution. Sampling must be sufficiently frequent to capture critical dynamics without loss of information. For instance, a dynamic process described by a periodic waveform (e.g., the oscillation of chromosomes) must be sampled at no less than the Nyquist frequency, which is defined as twice the highest frequency in the original waveform. Discrete sampling below the Nyquist frequency results in misestimation of the original waveform's frequency. Temporal aliasing is a serious concern in live cell imaging of yeast because wide-field 3D microscopes are currently unable to capture an image stack in <1–2 sec. Thus, we cannot hope to follow a process with a frequency above 0.25–0.5 Hz.

IMAGE INFORMATION CAPACITY

The Rayleigh formulation for resolution assumes noise-free images. In reality, noise is a major determinant of both the detectability and resolvability of objects. For example, even if two point sources are resolvable by Rayleigh criteria, it may be impossible to distinguish them if the amplitude of the noise exceeds the depth of the minimum in the intensity profile. When considering the detectability of small, faint objects, it is also important to consider both the level of the noise and the blurring effect of the optics. We can consider the impact of noise on images in a general sense by thinking about a microscope simply as an information transfer system with three spatial (*x, y, z*) and one temporal channel. As first shown by Shannon, the information capacity, *C*, of such a system is $C = f \log(1 + \mathrm{SNR})$, where *f* is the continuous bandwidth of the microscope in all four channels. As the SNR falls, the information capacity (the information about the image that can be conveyed by the microscope) falls and is completely lost when the SNR reaches 0. The bandwidth is itself a function of the cutoff frequencies of the objective lens. To understand why this cutoff exists, recall that a lens decomposes an image into its frequency components such that the lowest-frequency components (those containing the least detail) are toward the center of the optical axis and the higher-frequency components (those containing more image detail) are toward the edge (Fig. 3). Thus, as the half-angle (<θ>) of collected light increases, so does the objective's ability to collect higher frequencies and better resolve small objects. Viewed in another way, the fixed diameter of the objective limits the maximum frequency that can pass, the cutoff

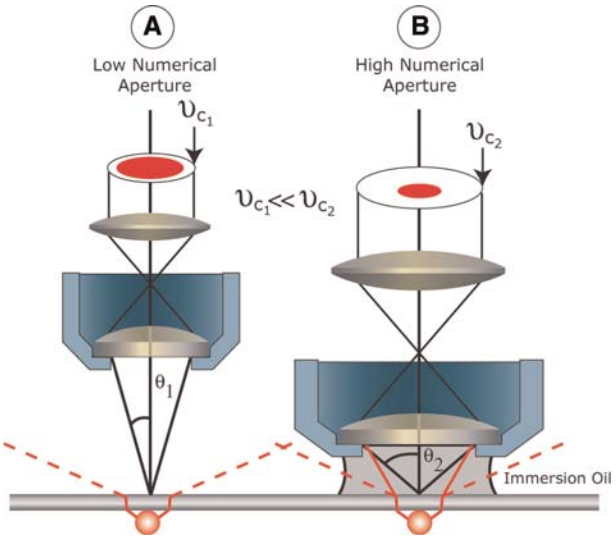

FIGURE 3. Comparing light collected from different NA objectives. Shown are two lenses with different NAs (low NA on the *left*, high NA on the *right*). Black lines represent half-angle cone of light collected by the objective as determined by the NA of the lens; the greater the half-angle (<θ>), the larger the NA value. The lens on the *left* (*A*) has a smaller NA than the one on the *right* (*B*); thus, $e_1 < e_2$. (Red dashed lines) Normal dispersion of emitted light from a single fluorescent point source after passing through a coverglass. Note that higher-NA objectives collect more light emitted from sample. In addition, use of refractive matched immersion oil limits excess refraction and enhances the number of photons collected by an objective (solid red line). The effects on image detail are illustrated about each objective with respect to the cutoff frequency. The higher-NA lens produces a more defined image, because it can collect the higher frequencies not available in the low-NA lens.

frequency, *Vc*, to an extent that varies with <θ>

$$v_c = \frac{2\text{NA}}{\lambda}, \text{NA} = n(\sin\theta).$$

All frequencies larger than *Vc*, which would define the fine structures of the object, are not conveyed by the objective lens and therefore cannot appear in the image (n = refractive index of medium). The precise relationship between resolution and SNR depends on specific properties of the image and the way it is processed, but a typical result from point object tracking is shown in Figure 4. The important point here is that it is ultimately both the cutoff frequency of the objective lens and the SNR that limit resolution and detectability under low-light conditions. Factors in the imaging system that affect SNR are discussed in detail below.

BRIGHTNESS

An additional question that is frequently asked, and one of particular relevance for live cell imaging, is how bright an object must be to be detectable. Detectability increases with the intrinsic brightness (*B*) of the object being imaged and the SNR of the image. Increasing the SNR is a significant problem in live cell imaging, because photobleaching and photodamage prevent us from increasing the intensity or duration of the illumination indefinitely. Instead, we must ensure that incident (excitation) photons are efficiently converted into fluorophore (emitted) photons. In other words, as many emitted photons as possible need to be collected by the objective and passed through the microscope to the camera, and the camera must be optimally configured to convert these emitted photons into an electronic signal. We consider each of these issues in turn, and in all cases concentrate on epifluorescence imaging.

The intrinsic brightness of a fluorescently tagged object depends on the number of fluorophores per unit volume (density), the probability that an excitation photon will be absorbed (the extinction coefficient of the fluorophore), and the probability that a photon will be emitted by the fluorophore in

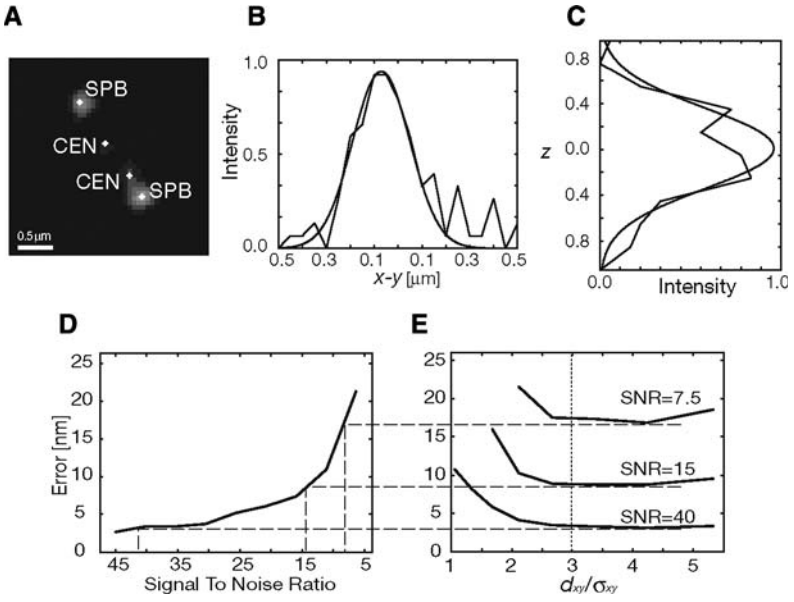

FIGURE 4. Dependence of localization error and resolution on SNR in a typical application. (*A*) Maximum intensity projection of an *S. cerevisiae* mitotic spindle. Spindle pole bodies (SPBs) are marked with GFP-tagged Spc42p, and the centromere proximal DNA is marked on chromosome III (CEN) with a TetO/TetR GFP-tagging system (Straight et al. 1996; Ciosk et al. 1998). (*B*) Gaussian approximation of the PSF for a fluorescent point source in the *x-y* plane. (C) Same as *B* with respect to the *z* plane. Note that distribution of Gaussian is greater in the *z* plane compared to the *x-y* plane. The combination of the two approximations describes the shape of a fluorescent point source in 3D. (*D*) The error in localizing a single-point source object as a function of the SNR. (*E*) The localization error as a function of the point-to-point distance calculated for three different SNR values. Note that the horizontal axis points from high to low SNR. The graph confirms the well-known fact that center positions of features with a known intensity distribution, in our case the distribution of the PSF, can be determined with sub-20-nm precision (Bobroff 1986). For SNR >15, the precision even reaches the single-nanometer range. With shorter separation distances, the accuracy decreases; the Rayleigh limit is denoted by a dashed vertical line. *dxy* is the separation distance between two spots and σ*xy* is the width of the Gaussian distribution. (*D* and *E*, Reprinted, from Thomann et al. 2002 with permission from Wiley © 2002.)

response to an absorbed photon (the quantum yield). It is also important to consider the difference between the excitation and emission wavelengths (the Stokes' shift). When the excitation and emission wavelengths are close, it is difficult to block all of the excitatory photons and collect only the much less numerous (~10^{-6}-fold) emitted photons. GFP has a relatively small extinction coefficient, quantum yield, and Stokes' shift when compared to chemical fluorophores, but some GFP variants are better than others (Tsien 1998). Moreover, enhanced GFP has good photostability, making it the best fluorophore for live cell imaging. Preliminary evidence also suggests that the intrinsic brightness of a protein can be increased considerably by fusing it to two tandem GFP tags. When deciding what proteins in a multiprotein complex to label, it is also helpful to choose those that are concentrated in a small area (for simplicity, we are ignoring possible complications from proximity-induced fluorescence quenching). Thus, to track the growth and movement of mitotic spindles in living cells, we decided to GFP-tag Spc42p, a protein that is present in many copies at the spindle pole bodies, rather than tubulin, which forms extended microtubule-based structures (Fig. 4A). The spindle pole bodies are smaller than the diffraction limit of the microscope (~0.24 µm) (Bullitt et al. 1997) and therefore appear as bright spots, independent of magnification. It is relatively simple to determine the center of these fluorescent spots and thereby measure the length and orientation of the spindle (Fig. 4B,C). In contrast, it is difficult to measure with precision the extent of tubulin in the spindle.

Choosing an Objective

Although many aspects of a microscope's optics affect the brightness of a feature, none are as important for fluorescent imaging as the NA of an objective lens (Fig. 3) (for review, see Spector and Goldman

2003). The observed brightness of a fluorescent image (*b*) is

$$b \approx B\left(\frac{NA^4}{M^2}\right)E,$$

where *B* is the fluorescent brightness of the object, *M* is the magnification, NA is the objective lens's numerical aperture, and *E* is the transmission efficiency of the optics. All other factors being equal, it is important to use the highest-NA, lowest-magnification lens available. In the case of diffraction-limited point-source objects, magnification does not affect brightness. As a practical matter, all high-NA microscope objectives are also high magnification and are typically available with 60–100× magnifications. For yeast, a 100× 1.4 NA lens is usually optimal. With regard to the transmission efficiency of the optics (*E*), it is important to avoid objectives designed for phase contrast, because the phase ring causes ~30% reduction in transmission. Similarly, it is important to remove differential interference contrast (DIC)-phase plates and prisms from the optical path, because they also reduce light transmission by as much as 70%. Fully color-corrected flat-field (Plan-Apochromat) objectives typically exhibit 75%–85% transmission for 400- to 700-nm light. It is possible to increase the transmission by a small but significant extent by using less than fully color-corrected objectives. Overall, the rule in live cell imaging is to use the highest-NA objective that is designed for epifluorescent imaging, rather than for phase contrast.

Filters and Dichroic Mirrors

To select the desired excitation and emission wavelengths, epifluorescence microscopes make use of three optical elements: an excitation filter, a dichroic mirror (beam splitter), and an emission filter. A typical arrangement is detailed in Figure 5, and a full range of absorption spectra can be downloaded

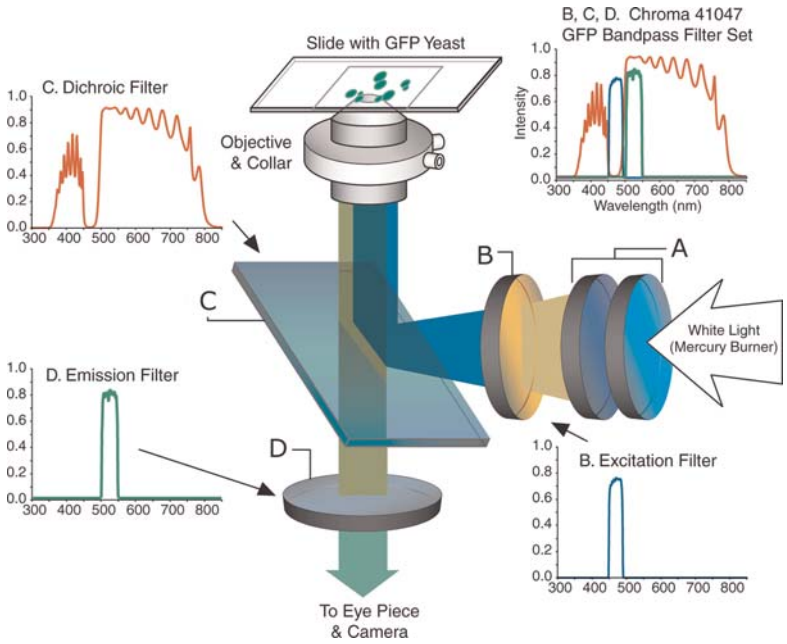

FIGURE 5. Filtering elements in a typical epifluorescent microscope system. (*A*) Light consisting of all wavelengths from the visible spectrum enters a set of neutral-density, UV, and infrared filters to block excessively damaging light rays. (*B*) Wavelengths are then filtered by passing through the excitation filter. Only those photons between 450 and 500 nm pass through this filter before being reflected by the angled beam splitter (dichroic) to the objective lens and to the specimen slide. (*C*) The beam splitter not only selectively reflects photons from the excitation wavelength, but also allows photons emitted from the specimen to pass directly through. In this example, only those photons between 450 and 500 nm are reflected. The photons emitted from the GFP molecules (510–530 nm) and any background fluorescence pass down through the splitter toward the emission filter. (*D*) Light slipping through the beam splitter is selectively blocked so that only those photons between 500 and 550 nm are passed through to the eyepiece or CCD (charge-coupled device) camera. Thus, the emission filter helps to reduce autofluorescent signals and excitation wavelengths that slip through the beam splitter. The graph of Chroma 41047 shows the overlapping image spectra from each of the individual elements for the GFP bandpass filter set.

from Chroma Technology Corp., Omega Optical, and other vendors. Broad-spectrum light from the mercury or xenon burner first passes through a series of infrared and UV-blocking filters near the rear of the microscope (Fig. 5A), and then through an interference filter that allows only excitation wavelengths to pass (Fig. 5B). Excitatory illumination is then reflected by the dichroic mirror toward the objective lens and the sample (Fig. 5C). Emitted photons from the sample are collected by the objective and pass through the dichroic and then through an emission filter on their way to the camera or oculars (Fig. 5D). Filter manufacturers such as Omega Optical (https://www.omegafilters.com) and Chroma Technology Corp. (http://www.chroma.com) offer filters in sets suitable for various applications. In many cases, all of the optical elements are mounted in a single holder known as a filter cube. In microscopes with automatic wavelength selection, the dichroic mirror is mounted in the cube, whereas the excitation and emission filters are mounted in separate motorized wheels.

We have encountered a considerable degree of confusion surrounding the selection and assembly of filter sets. The issue is easy to understand, however, if one makes reference to spectral plots and the geometry of an epifluorescence microscope (Fig. 5). Wavelength filtering in epifluorescence microscopes relies on a special property of dichroics: They reflect light shorter than a characteristic wavelength but are transparent to longer wavelengths (polychroic beam splitters have several transitions between reflection and transmission). Short-pass and long-pass emission and excitation filters are described by a wavelength that denotes the point of inflection between transmission and absorption (Fig. 6A,B). Alternatively, bandpass filters are described by the wavelength of peak emission (the center wavelength) and the width of the allowable band (the full width at half-maximum transmission; e.g., 520/20). By examining the characteristics of each element in a set, it is possible to choose sets for a particular application, but some experimentation with individual elements is advisable to fully optimize the optical train.

Live cell imaging of GFP-labeled yeast cells presents some special problems in filter set design and a trade-off must be made between sensitivity and selectivity. Because the Stokes' shift of GFP is small, it is common to pass all of the emitted photons from the sample while sacrificing somewhat on the excitation side. In some yeast strains, autofluorescence is a significant problem and filter sets must be assembled by the user to minimize the background. We have found that a long-pass GFP (Chroma, HQ500LP) emission filter provides good sensitivity for single-color recording of yeast cells expressing enhanced GFP. When autofluorescence is a problem, particularly with *ade*$^{-}$ strains (see below), use of the bandpass GFP (Chroma, HQ525/50m) emission filter is preferred. In dual-color imaging, filter and fluorophore combinations must be examined closely for overlapping wavelengths. However, combinations with cyan fluorescent protein (CFP)/GFP or CFP/YFP (yellow fluorescent protein) are usually quite successful. It is best if the less-abundant protein is tagged with GFP, because GFP is significantly brighter than CFP and is less likely to photobleach. It should also be noted that CFP and YFP can be used as a FRET (fluorescence resonance energy transfer) pair.

The shortest exposures and lowest possible illumination should be used for live-sample excitation. With our GFP-labeled spindles and tagged chromosomes, we typically collect 50-msec exposures per *z* section and use neutral density (ND) filters to reduce the incident illumination fivefold to 10-fold. A broad range of neutral density filters are available and should be kept on hand for this purpose.

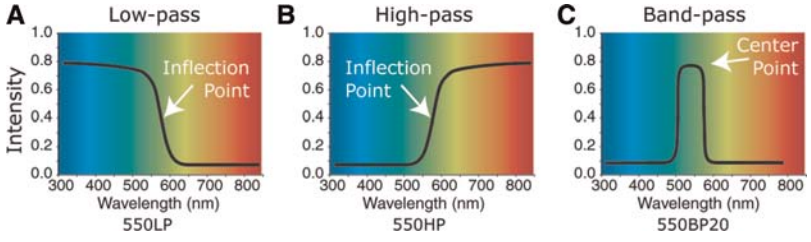

FIGURE 6. Filter types. (*A*) Low-pass filter selectively allows only wavelengths below 550–600 nm to pass in this example. Longer-wavelength photons are blocked by the element. (*B*) High-pass filter designed to allow wavelengths above 550–600 nm to pass through. (C) Bandpass filter blocks both short and long wavelengths while allowing only light from 525–625 nm to pass through.

Camera design and configuration are critical variables in determining the brightness of images and the extent to which features can be discriminated. Because they are invariably more efficient than color cameras, we consider here only the monochromatic charge-coupled device (CCD) cameras. In a microscope system connected to a monochromatic camera, exposures are taken with different excitation and emission filters and color is introduced after the fact by assigning a hue to each exposure based on the properties of the filter. The construction of CCD cameras is a relatively complex topic that we will not cover in any detail, but to optimize camera performance, it is helpful to have a basic understanding of their operation (Fig. 7). At the core of a CCD camera is a chip containing a rectangular area of photosensitive detectors—pixels—that convert photons into electrons with a particular quantum efficiency (QE, which varies with wavelength and is typically 60%–80% for blue-green light). After an exposure is taken, the number of electrons generated at each pixel is determined by an analog-to-digital converter (ADC). Cameras typically have only one ADC and the electrons in each pixel of the CCD must therefore be moved to the ADC via a series of positional shifts, until the entire chip has been read (Fig. 7). Thus, even though a CCD camera collects photoelectrons at each pixel in a parallel process, the pixels are read serially. Serial readout significantly limits the rate at which CCD cameras operate, and thus the fewer the number of pixels read, the greater the rate at which successive frames can be recorded (commonly referred to as frame rate). One simple way to increase frame rate is to limit the area of the CCD being read by the ADC. Yeast cells are sufficiently small, even with a 100× objective, where a 64 × 64-pixel or 128 × 128-pixel area of the CCD is usually sufficient. A second method to increase frame rate is to add the contents of adjacent pixels together prior to their arrival at the ADC in a process known as on-chip binning. Besides faster readout, binning increases the SNR at the cost of lower image resolution. To understand the impact of binning on an image, note that the pixels in a CCD array perform a discrete sampling of the image, which is a continuously varying two-dimensional waveform. The pixel array must therefore, by Nyquist criteria, sample the image at twice the frequency of the highest spatial frequencies in the image. The highest frequency in the image is determined by the cutoff frequency *Vc* of the objective. We can therefore determine the pixel spacing, *px*, as follows:

$$p_x \leq \frac{\lambda M}{4\mathrm{NA}}.$$

With a 100× 1.4 NA objective, the largest acceptable pixel spacing is 8.9 µm. For instance, a Roper CoolSNAP HQ interline CCD camera has a pixel size of 6.25 × 6.25-µm without binning, and

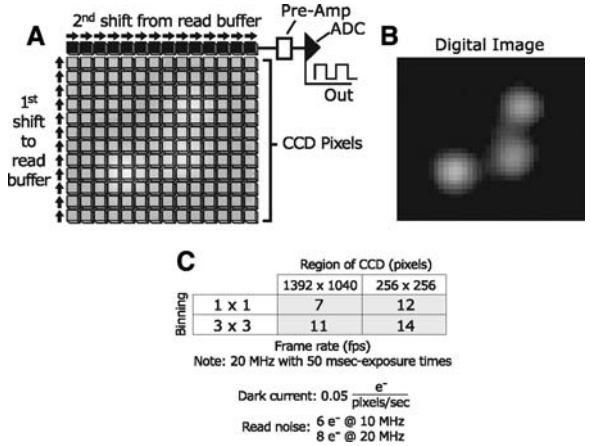

FIGURE 7. CCD chip architecture. (*A*) Photons coming from the microscope hit the surface of the CCD photosensitive detectors. These photons are registered and incrementally counted as electrons for the desired exposure duration. The electron count is converted into signal intensity by a single read buffer (ADC) at the *top* of the array. To read each line from the CCD array, the information must be shifted up one line at a time until the entire image is transferred into the read buffer and read out sequentially. (*B*) Once complete, the raw digital image can be reconstructed from the individual intensity values. (*C*) Properties of a typical high-performance interline CCD camera.

with a 100× 1.4 NA objective lens, oversamples the image 1.4-fold (relative to the Nyquist criteria). This is reasonable for small diffraction-limited objects. In contrast, 2 × 2 binning (to create 12.5 × 12.5-μm superpixels) would be detrimental.

CCD cameras are subject to three sources of noise: dark noise, photon noise, and read noise. Dark noise refers to the random generation of electrons, within the photosensitive elements of the CCD array, from heat rather than by photon absorption. Modern microscope cameras cool the CCD to between −30°C and −50°C, effectively making dark noise negligible. Photon noise, also known as shot-noise, arises from variations in the flux of photons in a beam of constant intensity. Photon noise exhibits Poisson statistics, varying with the square root of the signal, and is an intrinsic feature of photons that cannot be eliminated by changes in camera design and setup. Read noise refers to uncertainty in the measurement of photoelectron number introduced by limitations in the preamplifier, ADC, and other electronics in the camera (http://www.roperscientific.com). Read noise is a function of the quality of the camera and the care that has been taken in designing the electronics, but for a given camera, the faster the read rate of the camera, the greater the noise. Ideally, imaging should be performed under conditions in which the physics of photon counting and not the camera design is limiting. Under these conditions, commonly referred to as photon-limited imaging, photon noise is the greatest contributor to overall noise. However, it is not always possible to work in this range with live samples, and we typically find ourselves recording in the instrument-limited range. Under these circumstances, it is important to find the lowest-noise cameras and lowest-noise settings. For example, with a CoolSNAP camera recording 50-msec exposures on a 128 × 128 area of the CCD, we have observed a dramatic increase in SNR but little decrease in frame rate by dropping from a 20-MHz read rate to 10 MHz.

In summary, for live cell imaging of yeast, it is usually best to use only a fraction of the area of a megapixel CCD camera. This makes it possible to increase the frame rate while keeping the ADC read rate as low as possible to increase SNR. In general, avoid binning the image, but before accepting this nostrum, it is best to perform the simple calculation mentioned above to see if this is also true for the microscope being used. If it allows binning, then the image SNR will increase, because the signal becomes photon-noise-limited at a lower overall intensity. Before leaving the topic of cameras, however, it is worth mentioning interline CCD architectures, which have a significant impact on frame rate. In an interline CCD, a set of masked (nonphotosensitive) pixels are interleaved between the primary photosensitive detector lines. Such interline CCDs have a primary recording array and a second masked array. An entire frame can be shifted in parallel from the recording to the masked array, and the masked array can then be digitized while the primary array is recording a subsequent exposure. This makes it possible to record successive frames without a shutter. Historically, interline CCDs have had the drawback that the interline masks reduce the fraction of the chip that responds to light and therefore reduce camera sensitivity. Recent cameras circumvent this problem by including a small lens for each pixel that focuses the light from masked elements onto photosensitive elements, thereby achieving both increased speed and increased sensitivity. Interline CCD cameras currently represent the best option for high-speed live cell imaging (Fig. 7C).

PREPARING AND MOUNTING SAMPLES FOR LIVE CELL IMAGING

Quite often the most tedious parts of live cell microscopy are keeping cells growing proficiently and preventing them from floating around during an imaging session. The following sections describe procedures for selecting appropriate strains, preparing the culture, and maintaining cells in a suitable environment.

Strains and Growth

Autofluorescence can be a significant problem in yeast if cultures are grown under poor conditions, especially when working with ade$^-$ strains. In ade$^-$ strains, a colored intermediate in adenine biosynthesis, phosphoribosylaminoimidazole, accumulates to high levels in the absence of exogenous adenine and is highly fluorescent when excited with blue light (Stotz and Linder 1990). In fact, it is the phosphoribosylaminoimidazole that gives ade$^-$ yeast cells the distinctive red color used in genetic sectoring assays (Ishiguro 1989). Autofluorescence can be minimized by using ADE$^+$ genetic backgrounds and growing cells in synthetic complete (SC) medium supplemented with essential amino acids and 20 μg/mL extra

adenine. Additionally, cultures should be maintained below 5×10^6 cells/mL for 4–10 generations, and the medium should be refreshed prior to mounting and imaging.

Slide Preparation

Although it is possible to mount live yeast cultures directly under a coverglass, we have found it quite difficult to avoid physical damage and to hold cells in a fixed position using direct mounting. Thus, we recommend mounting cells on a pad of 1.2% agarose formed in a slide that contains a shallow depression. This system not only holds the cells in place better and prevents accidental shearing, but it also provides cells with a significant volume of nutrients to help maintain cell viability. The use of agarose pads is particularly important for time-lapse experiments, and we have successfully used them to maintain cells at wild-type growth rates for 8 h or more (Fig. 8).

Preparing Slides with an Agarose Cushion

1. To prepare the agarose solution, combine 10 µL of SC medium supplemented with a Complete Supplement Mixture of amino acids (Bio101, http://www.Bio101.com), 20 µg/mL of additional adenine, and a carbon source (e.g., 2% w/v glucose) with 1.2% (w/v) agarose. Heat the solution in a microwave to completely melt the agarose.
2. Add 200 µL of melted agarose solution to a 60°C prewarmed slide fabricated with a shallow 18-mm hemispherical depression (VWR, http://www.vwr.com) (Fig. 9A). Quickly cover the agarose-filled depression with a regular microscope slide (the top slide) by placing it directly onto the agarose. Using the thumbs, press evenly against the top slide for 1 min to allow the agarose to harden (Fig. 9B).

   Excess agarose will squeeze out from the edges. It is essential that no air bubbles be trapped in the agarose during this process and that the agarose forms a smooth flat surface with the slide. To prevent dehydration, leave the top slide in place until cells are ready for mounting.
3. Prepare a 22 × 22-mm, no. 1.5 (0.16- to 0.19-mm), coverglass (VWR) for mounting by first physically removing dust particles from the coverglass with a dry artist's paintbrush and hand blower (e.g., Bergeon Dust Blower from http://www.watchpartsusa.com or http://www.nationaljewelerssupplies.com). Make sure to remove any particles from the coverglass since they will prevent a tight seal with the agarose pad.

Avoid using precision wipes (e.g., Kimwipes) as they can leave scratches and fluorescent strands on the glass. In addition, avoid Dust-Off or similar compressed gas products because they usually contain small, highly fluorescent particles.

The coverglass is an important and often overlooked component of the optical path. Objective lenses are typically designed to work with a particular thickness of coverglass, usually no. 1.5 (0.16–0.19-mm thickness), and proper selection can enhance image quality. For the most precise work, it is good practice to measure the thickness of the coverglass and to use only those within ±0.02 mm of

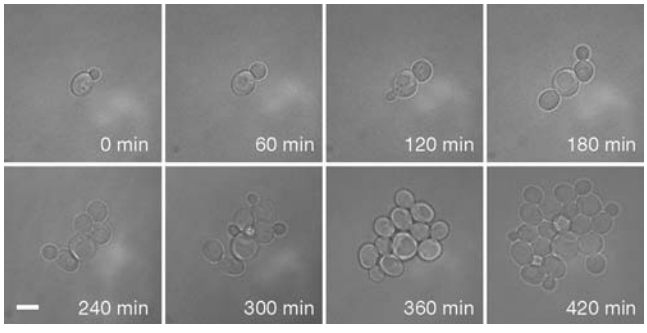

FIGURE 8. *S. cerevisiae* cells growing on an agarose specimen slide. Wild-type cell culture grown in medium to log phase and mounted at 1×10^7 cells/mL using the techniques described in this article. The slide was maintained at 30°C for just over 8 h. Series of phase-contrast images collected at regular intervals (every 60 min) to monitor growth rates. Culture doubles every 90–100 min based on cell counts. Bar, 4 µm.

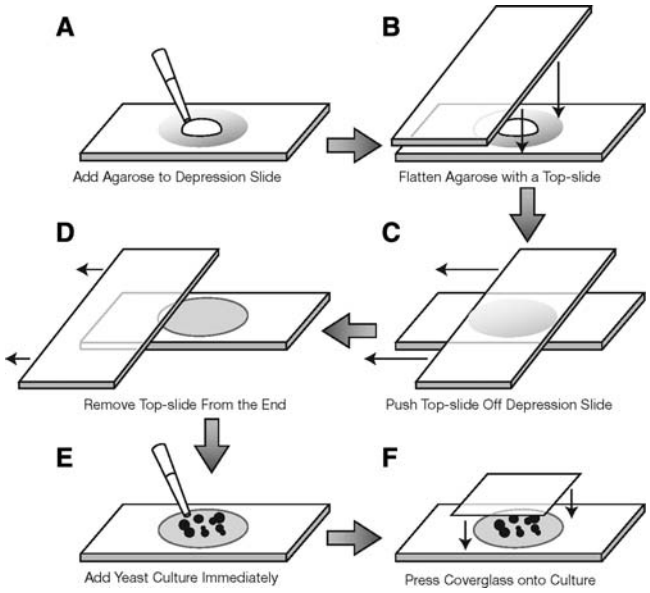

FIGURE 9. Preparing specimen slide with agarose pad and mounting of *S. cerevisiae* cells. (*A*) 200 µL of hot agarose/SC-Complete Medium Mixture is added to a 60°C prewarmed depression slide using a pipette. (*B*) A prewarmed *top* slide is placed directly on the agarose-filled depression and pressure is held evenly across the *top* slide for 60 sec while the agarose solution hardens. (*C*) The *top* slide is gently removed by sliding it toward one end of the depression slide. (*D*) After removal of the top slide, excess agarose is removed from the depression slide to create a flat and even surface. (*E*) 2.2 µL of yeast culture is immediately added to the center of the agarose pad using a small pipette tip. (*F*) A dust-free petroleum-edged coverglass is gently placed on *top* of the yeast sample and sealed by applying light amounts of pressure to the four sides of the coverglass. Large air bubbles can be removed by gently applying pressure to the coverglass in a radial direction.

nominal dimension. A digital micrometer suitable for measuring thickness can be obtained from any tool supply house (e.g., http://www1.mscdirect.com).

4. Apply a very fine band of 100% pure petroleum jelly (e.g., Vaseline) to the extreme edge of the coverglass. Do this to all sides by adding a very small amount of jelly with a toothpick to one corner and running a finger gently along the extreme edge to distribute the petroleum jelly evenly.

   The petroleum jelly prevents rapid evaporation of the cell culture medium and creates a better seal when the coverglass is applied to the agarose bed.

Mounting Cells

5. To pellet the cells, transfer 1 mL of log-phase yeast culture to a microcentrifuge tube and centrifuge at low speed (4000 rpm) for 1 min. Avoid overspinning.

6. Remove the supernatant from the microcentrifuge tube and resuspend the cell pellet in 0.3–0.5 mL of fresh SC medium (as in Step 1 but without agarose).

   The volume used to resuspend the cells depends on the size of the cell pellet in Step 5 and the desired final cell density on the microscope slide.

7. Remove the top slide to expose the agarose pad by gently pushing the top slide along the length of the depression slide (Fig. 9C,D). This step should release the seal between the two slides and leave a very smooth surface on top of the depression slide. If any large bits of agarose remain, carefully remove them.

8. Transfer 2.2 µL of resuspended cell culture to the smooth agarose and gently place the coverglass with petroleum jelly over the cell culture (Fig. 9E,F). To create a tight seal, apply a very slight amount of pressure at the extreme edges of the coverglass. Do not press too hard because the cells could be damaged or crushed between the coverglass and microscope slide.

9. Spot a small amount of nail polish at the four corners of the coverglass to prevent it from sliding or pulling away from the agarose bed during the imaging session.

INSTRUMENTATION: ENVIRONMENTAL CONTROL AND MICROSCOPE OPTICS

Environmental Control Devices

Temperature-sensitive yeast strains are well suited to live cell microscopy and present an opportunity to determine the role of a single gene on a dynamic process in a living cell. However, special consideration must be given to control the temperature of the yeasts' environment, because the objective and slide are coupled thermally via immersion oil, and thus the objective acts as a heat sink. Live cell yeast microscopy can be performed successfully on either upright or inverted microscopes, and commercial environmental control systems are available for both. With yeast cells, it is not necessary to use the elaborate chambers developed for animal cells, because the regulation of oxygen and CO_2 levels is not critical. When choosing or building an environmental control system, it is important to keep in mind the geometric constraints imposed by high-NA objectives. These include a relatively large-diameter lens, direct contact with the sample (via immersion oil), and short working distance. In our experience, by using a stage heater, an objective heater, and the depression slide system discussed in the previous section, it is possible to maintain live yeast cells at temperatures from 15°C to 40°C for many hours. The best way to perform rapid shifts from permissive to nonpermissive temperatures is to use preheated objectives, rather than to change the temperature of a single objective. Note that such a shift entails a compromise in the choice of mounting oil (see below).

Building a Thermally Regulated Slide Holder

A simple stage heater can be fabricated from a brass block measuring 4 × 2 × 0.5 inches. One advantage of this simple water-based thermal system is that it appears to be more stable thermally than traditional resistive systems, which cycle on and off. In addition, a refrigerated circulator allows cold-sensitive mutants to be chilled below room temperature.

A completed thermal unit should make clean contact with the microscope objective and look similar to the detailed arrangement shown in Figure 10D (e.g., inverted microscope configuration).

1. Drill a 1-inch hole through the block to permit bright-field illumination. Drill intersecting holes through the length of the block, cap them with seals, and connect the block via tubing to a circulating water bath to create a continuous channel for heated or cooled water (Fig. 10A).
2. Fit a temperature collar (available from Bioptechs Inc., http://www.bioptechs.com) over the objective to regulate its temperature (Fig. 10B) and to prevent heat from being absorbed into the microscope base. Exercise caution in using the collar since it is typically wide enough that excessive stage movement can cause the objective to crash into the stage.
3. Insert small spring-steel clips to hold the slide firmly to the brass block and ceramic foot pads to prevent heat loss through contact with the microscope stage (Fig. 10C).

Commercial Environmental Systems

Commercial temperature-control systems are available in a wide range of configurations, styles, options, and price ranges. Some systems are similar to the basic system described above and contain nothing more than an aluminum slide holder connected to a resistive heating coil (http://www.instec.com). Others, typically designed for mammalian cell microscopy, are elaborate temperature-regulated circulating dishes (http://www.bioptechs.com). These systems are not well suited to yeast work, because most mammalian studies use adherent cells that bind tightly to the coverglass, whereas yeast cells float or spin around continuously. Finally, acrylic chambers that enclose most of the microscope are also available and can be used to control the air temperature as well as that of the microscope (http://www.lis.ch/thebox.html). This type of system has the advantage of keeping the entire microscope, stage, and objective at the desired temperature, but the cost is significantly greater than a stage-mounted controller. Regardless of what system is used, the temperature of the slide must be monitored as close to the sample as possible using a small thin-film RTD temperature sensor and a digital thermometer (http://www.omega.com). We find that the actual temperature of the sample typically differs by 1°C–3°C from the temperature of the circulating bath.

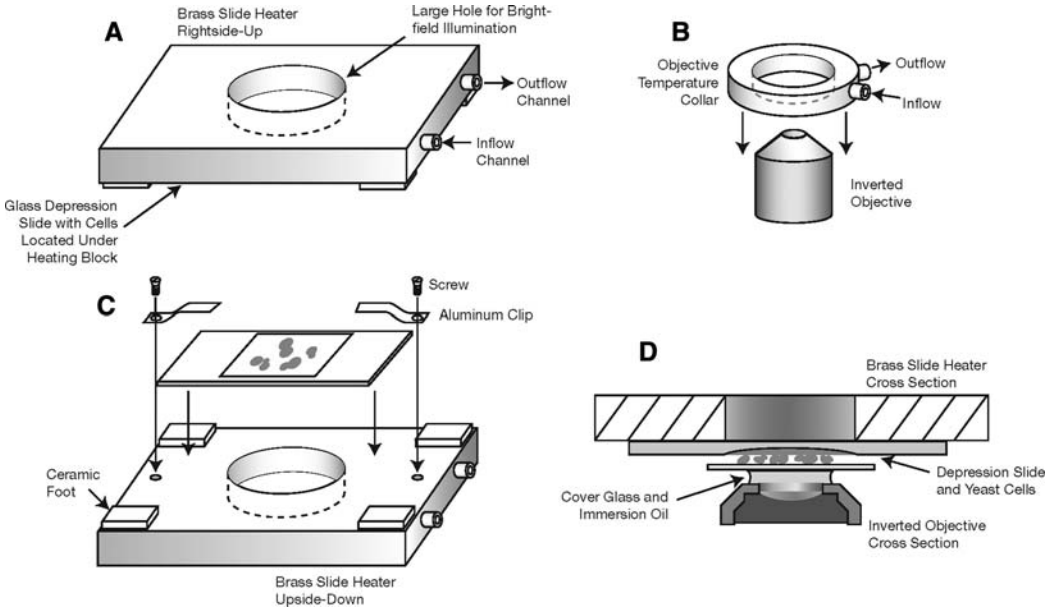

FIGURE 10. Temperature controller block and objective lens assembly. (*A*) Liquid-controlled thermal block for maintaining specimen slides at desired temperature. Channels through the block allow liquid to flow in through one port and out the other. The block can be fabricated with a large hole bored directly through the center to allow bright-field illumination on the specimen slide (normally attached to the *bottom* of the block for inverted microscope configurations). Flat ceramic blocks can be added to the *bottom* of the block to insulate the block and specimen slide from the microscope stage. (*B*) Commercial liquid-regulated thermal collar for an objective lens. The ring is incorporated into the liquid circulating system, typically provided from a temperature-controlled circulating water bath. (C) Thermal block in upside-down configuration. Small aluminum clips and screws are used to hold the specimen slide to the underside of the block for inverted microscope configurations. Screws and clips can be added to the *top* of the block for upright configurations. (*D*) Fully assembled thermal block with specimen, slide, and mounting oil placed over inverted microscope objective.

Limiting Geometric Aberrations

Imperfections in lens geometry or sample mounting directly affect the shape of the PSF in distinct ways (Fig. 11). A tilted or misaligned lens skews the PSF so that it is no longer perpendicular to the optical stack or is bent in half (Fig. 11B). A PSF of this type suggests a significant problem with tilt and centration in the

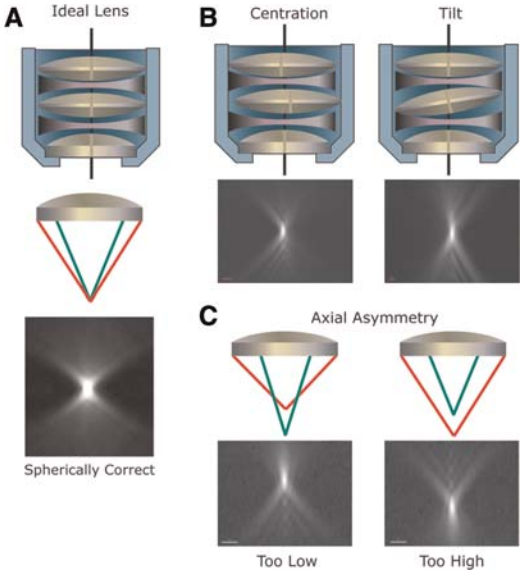

FIGURE 11. Lens aberrations and spherical aberration. (*A*) An ideally shaped lens should collect photons symmetrically from a single focused point shown by the red and green lines. With the correct immersion medium, the light from a single fluorescent point source results in a spherically correct or symmetric PSF. (*B*) Improperly aligned elements within the objective lens results in PSF deformation. A lens can be misaligned laterally (e.g., centration) or in a slightly tilted configuration. Lens construction problems cause the PSF to be altered perpendicular to the *x*-*z* plane or bent asymmetrically about the point source origin. (*C*) Aberrations in the PSF can also occur when imperfections in the curvature of the glass cause light to be collected from different axial-shifted positions in space and result in axial asymmetry (also known as spherical aberration). Spherical aberrations can additionally result from using an immersion oil with the wrong refractive index. All aberrations lead to a reduction in the signal intensity strength and distortions in the final image.

objective and cannot be corrected by the user. When the PSF symmetry is disrupted in the longitudinal or axial dimension (Fig. 11C), spherical aberration is the problem. Spherical aberration can arise from problems with the objective or the use of immersion media with the wrong refractive index. The small size of a yeast cell relative to the resolution limit of an optical microscope requires that spherical aberration be minimized, because even small axial aberrations lead to relatively large errors. Spherical aberration can be reduced dramatically by selecting an immersion medium with the proper refractive index.

Refractive Index Matching Using Immersion Media

Immersion lenses are designed to work with either oil- or water-based media but not both, as specified on the side of the lens housing. The higher the refractive index of the immersion oil, the greater the extent to which light is bent into the objective; therefore, the highest-NA lenses are oil immersion (see Fig. 3). Environmental factors, particularly temperature, affect the refractive index of the mounting and immersion medium, and mismatches in either cause spherical aberration. By changing the refractive index of the immersion medium within a narrow range, it is possible to correct for differences in the culture medium, coverglass thickness, and temperature. Kits with immersion oils having refractive indexes between 1.500 and 1.534 in increments of 0.002 can be obtained from Applied Precision (http://www.api.com) or Cargille Laboratories (http://www.cargille.com). Choosing which oil to use for a given temperature is determined empirically, based on a visual analysis of the PSF with different oils. When the angle of light dispersion is greater above the point source than below it, the refractive index of the mounting medium is too high and vice versa (Fig. 11C). When the PSF is nearly symmetric in *z*, the correct refractive index must be determined. We find that when imaging live yeast at 30°C with no. 1.5 coverglass, a refractive index of 1.518 is typically appropriate; at 37°C, the correct refractive index can be as high as 1.526 or 1.528. Although oil matching can be tedious at first, the process becomes routine over time and the results are worth the effort.

Experimental Determination of PSF

Determining the PSF of an objective under typical imaging conditions can help to identify flaws in the objective and problems with sample preparation. The following protocol describes an approach for the experimental determination of PSF.

1. Dilute a set of small fluorescein isothiocyanate (FITC)-conjugated beads in the same medium as is used for mounting cells (SC medium supplemented with a Complete Supplement Mixture of amino acids [Bio101 (http://www.Bio101.com)], 20 µg/mL of additional adenine, and a carbon source).
2. Add 2.2 µL of the bead mixture to a coverglass coated with poly-L-lysine, and seal it with nail polish onto a standard microscope slide.

   An initial immersion oil with a refractive index of 1.516 is a good starting point for imaging at room temperature.
3. While focusing the lens above, through, and beyond the point source (using the motorized system), collect sections at regular intervals (e.g., every 0.020 µm).
4. Examine by eye the symmetry and extent of blurring once the stack of optical *z*-sections are rotated up by 90° and viewed from the side (Fig. 11A).

   The spherically correct PSF is completely symmetric both above and below the point source as well as circularly symmetric.
5. Change the immersion oil refractive index until a symmetric PSF is obtained.

PHOTODAMAGE

As discussed above, phototoxicity and photobleaching are significant problems in live cell analysis. The exact mechanism of GFP photobleaching has not been elucidated. What is known is that the protein is neither destroyed nor degraded; rather, continuous or long-term repeated exposure to excitation wavelengths irreversibly alters the GFP molecule so that it can no longer fluoresce. This property can be utilized in fluorescence recovery after photobleaching (FRAP) experiments and is a common approach to studying cytoskeletal dynamics.

Phototoxicity indirectly describes a general class of harmful effects on live cells based on either long-term or short but extreme exposures to a light source. Phototoxicity is much more difficult to discern than photobleaching, because it is harder to measure directly and can be a consequence of DNA damage (UV light) or protein damage (infrared light). In addition, excessive excitation of a fluorophore can lead to oxide radical formation and may also negatively impact cell growth. To avoid unpredicted effects during live cell acquisition, it is important to incorporate interference filters into the microscope system. Quite often, multiple filters can be piggybacked on top of one another. Alternatively, special filters can be ordered that have the appropriate filters fused together (http://www.chroma.com and https://www.omegafilters.com). Performing 3D microscopy on cells exaggerates the negative effects of photobleaching and phototoxicity. The acquisition of multiple optical sections requires continuous or repeated exposure by a magnitude based on the number of sections taken. Consequently, performing live cell analysis with fluorescent light mandates attention to detail and proper microscope configurations.

To minimize photobleaching, a bandpass excitation filter (e.g., Chroma, HQ470/40X) and an infrared-blocking filter can be combined in series with the emission filter to block unwanted infrared and UV irradiation. In addition, neutral-density filters can be used to reduce the intensity of excitatory illumination across all wavelengths. These filters are described by a number that increases in value as the percent transmission falls. Such filters are available from 0.100 (80% transmission) up to 3.0 (0.10% transmission). With all filters, maintenance is also required over time. This is especially true for those filters immediately exposed to an intense light source, such as excitation and neutral-density filters. We have found that these elements will fade, develop small imperfections, and experience pinhole defects over time and should be replaced after ~6 mo of heavy use.

The best exposure time and neutral-density filter combination must be determined empirically and depends on how frequently repeated exposure is required and on the dynamics of the process being imaged. We have found that 50 msec and a 0.500 neutral-density filter works best for rapid acquisition movies where 14–20 optical *z* sections are taken every 5 sec. This combination allows us to acquire a movie with 120 time points up to 10-min long using enhanced GFP-labeled spindle pole bodies and single chromosome tags.

FUTURE DEVELOPMENTS

During the next several years, expect important developments to occur in live cell microscopy and automated image analysis. Machine vision methods have the potential to greatly accelerate the rate at which image information can be converted into quantitative information for mechanistic and screening studies. In addition, machine vision methods can extend the resolution limit of microscopes beyond the Rayleigh limit and can process images that are too indistinct for human interpretation. Machine vision, therefore, has the potential to overcome many of the practical problems associated with live cell imaging, including phototoxicity and photobleaching, large data streams, and subjective data analysis.

WWW RESOURCES

http://www.chroma.com (Chroma Technology) Excellent online handbook of filter basics, GFP filter brochure, and absorption spectra

http://www.hamamatsu.com (Hamamatsu Photonics) Leading camera manufacturer

http://www.microscopy.fsu.edu (Molecular Expressions Primer) Excellent source of microscopy information; many interactive demos for understanding important concepts

https://www.omegafilters.com (Omega Optical) Curv-o-matic viewing of filter spectra online

http://www.roperscientific.com (Roper Scientific) Good technical library from a leading camera manufacturer

REFERENCES

Bobroff N. 1986. Position measurement with a resolution and noise-limited instrument. *Rev Sci Instrum* **57:** 1152–1157.

Bullitt E, Rout MP, Kilmartin JV, Akey CW. 1997. The yeast spindle pole body is assembled around a central crystal of Spc42p. *Cell* **89:** 1077–1086.

Ciosk R, Zachariae W, Michaelis C, Shevchenko A, Mann M, Nasmyth K. 1998. An ESP1/PDS1 complex regulates loss of sister chromatid cohesion at the metaphase to anaphase transition in yeast. *Cell* **93:** 1067–1076.

Inoue S. 1995. Microscopes. In *Handbook of optics*, 2nd ed. (ed. Bass M et al.), Vol. 2, pp. 17.1–17.50. McGraw-Hill, New York.

Ishiguro J. 1989. An abnormal cell division cycle in an AIR carboxylase-deficient mutant of the fission yeast *Schizosaccharomyces pombe*. *Curr Genet* **15:** 71–74.

Spector DL, Goldman RD. 2003. *Essentials from cells: A laboratory manual (Laboratory Essentials on CD)*. Cold Spring Harbor Laboratory Press, Cold Spring Harbor, NY.
Stotz A, Linder P. 1990. The ADE2 gene from *Saccharomyces cerevisiae*: Sequence and new vectors. *Gene* **95:** 91–98.
Straight AF, Belmont AS, Robinett CC, Murray AW. 1996. GFP tagging of budding yeast chromosomes reveals that protein–protein interactions can mediate sister chromatid cohesion. *Curr Biol* **6:** 1599–1608.
Thomann D, Rines DR, Sorger PK, Danuser G. 2002. Automatic fluorescent tag detection in 3D with super-resolution: Application to the analysis of chromosome movement. *J Microsc* **208:** 49–64.
Tsien RY. 1998. The green fluorescent protein. *Annu Rev Biochem* **67:** 509–544.